14. A STUDY OF THE PROBLEMS OF CONTROL OF A SUPERSONIC INLET

By John J. Gawienowski, and John L. Benson[1]
NASA Ames Research Center

SUMMARY

A major problem in operating internal contraction inlets on supersonic aircraft is preventing inlet unstart due to terminal shock instability. Factors contributing to this problem, such as the dynamic response of an inlet to internal and external disturbances and performance characteristics of inlet controllers, were investigated. The results of the investigation showed that for the given inlet design and its idealized control system, a stability margin corresponding to less than 1-percent reduction of pressure recovery would prevent inlet unstart by the simulated disturbances, and that the dynamic and static characteristics of the current state-of-the-art inlet controllers would adequately meet the requirements of a control system for a supersonic mixed-compression inlet. A comparison of an analytical inlet model with experimental results showed very good agreement.

INTRODUCTION

A major problem in the operation of a mixed compression inlet on a supersonic aircraft is inlet unstart due to terminal shock instability. To achieve high efficiency of the propulsion system it is necessary to maintain the terminal shock close to the inlet's aerodynamic throat. The necessary stability margin, the distance from the throat at which the terminal shock must be positioned to prevent unstarting, is a function of the amplitude and frequency of the flow disturbances, the dynamic characteristics of the inlet, and the response and static accuracy of the control system. To examine each of these factors, a research program was undertaken by Ames through a contract with the Lockheed-California Company. The program objectives are presented in figure 1. The research effort was divided into three major areas: the wind-tunnel testing of a controlled axisymmetric inlet to determine the response of the terminal shock when subjected to simulated internal and external disturbances; the bench testing of representative state-of-the-art inlet controllers to determine their performance characteristics; and finally, a comparison of the response of an analytical representation of the inlet system with experimental data. A detailed description of the test equipment, procedure, and results is presented in reference 1.

[1]Lockheed-California Company.

SYMBOLS

m_2/m_∞	engine-face mass-flow ratio
M_∞	free-stream Mach number
P_{12}	static pressure, on centerbody aft of throat
P_{t_2}/P_{t_∞}	engine-face total-pressure recovery
α	angle of attack

DESCRIPTION OF MODEL

The axisymmetric mixed-compression inlet model tested is shown in figure 2. The inlet incorporates three boundary-layer-bleed plenums on the centerbody and two on the cowl, and is instrumented with 45 dynamic pressure transducers and 281 static pressure orifices. The cowl sleeve can be translated to vary contraction ratio and the aft sleeve can be translated to regulate exit mass flow. Probes were located at the cowl lip to measure local Mach number. The measured steady-state performance of the inlet shown in figure 3 is representative of the current $M = 3.0$ inlet state of the art. The maximum pressure recovery is 88 percent with a bleed mass-flow ratio of approximately 8-1/2 percent.

Figure 4 is a schematic drawing of the inlet and its controls. The model is equipped with a variable bypass valve located at the simulated engine face station and a variable aft-exit valve. Both valves can be scheduled to perform various time-dependent displacements controlled from a small analog computer or a signal generator. The analog computer also served as an idealized inlet controller in a closed-loop shock position control system in which static pressure orifice P_{12} provided the control signal. For this control mode, the switches in figure 4 are closed. During this phase of the investigation, the bypass valve responded to an error signal proportional to the difference between the steady state and the disturbed shock position. The flow disturbances were generated internally by the aft exit valve and externally by the disturbance airfoil.

Figure 5 is a photograph of the airfoil installed in the Ames 8- by 7-foot wind tunnel. The airfoil has a rectangular planform which spans the test section. It is supported at the center by a strut mounted from the tunnel ceiling and at each tip by journal bearings which permit rotation in angle of attack. The airfoil is located far enough upstream for the inlet to operate in the "far" field produced by the airfoil when it is oscillated through angle of attack. The mechanism for oscillating the airfoil operates through the center strut.

DESCRIPTION OF DISTURBANCES

Figure 6 lists the internal and external disturbances investigated in the test program. The internal disturbances considered were: simulated engine disturbances, such as a throttle advance or afterburner blowout, and sinusoidal oscillations of the exit mass flow. These engine transients were chosen to be investigated because of their relatively large amplitudes and short periods. The time history variations of engine airflow were obtained from the General Electric Company. The external disturbances investigated were: a simulated atmospheric gust, a simulated shock wave from passing supersonic aircraft, and sinusoidal oscillations of the disturbance airfoil. The gust was investigated because it is believed to be the most common atmospheric disturbance, and because it is known to cause occasional large perturbations. It was treated as a discrete phenomenon with a cosine variation of Mach number representing a 1.5-percent change in local Mach number. Because it was not possible to vary wind-tunnel temperatures rapidly gusts due to free-stream temperature changes could not be simulated. The passing shock wave was investigated because it was believed to present the strongest probable external disturbance. The time history variation of external pressure, which represented a ±1 percent change in local static pressure, was determined from sonic boom measurements.

To obtain the inlet's dynamic characteristics the response of the inlet's terminal shock to sinusoidal oscillations of the exit plug or of the disturbance airfoil was determined before the engine and atmospheric disturbances were simulated. Data were obtained for exit plug frequencies from 1 to 30 cps and disturbance airfoil frequencies from 1 to 20 cps, with the inlet control in both open and closed loop modes.

Test results showed that for both internal and external sinusoidal disturbances the response characteristic of the inlet terminal shock was approximately linear up to 10 cps.

RESPONSE TO THROTTLE ADVANCE

Figure 7 shows the response of the inlet model to an engine throttle disturbance for both open and closed loop modes. This disturbance was simulated by a reduction in diffuser exit mass flow as shown in the upper plot. The open-loop control mode, with the bypass valve inoperative, is shown as a solid line; the closed-loop mode, with the bypass valve operative is shown as a dashed line. The resulting change in signal pressure, P_{12}, in pounds per square foot, is shown in the next plot. The response of the terminal shock position, in inches aft of the spike vertex, indicates that the closed-loop mode caused a significant reduction in terminal shock motion compared with the open-loop mode. All the simulated disturbance tests were made with the terminal shock initially positioned to prevent unstart in the open-loop mode. This procedure was adopted because earlier tests had indicated that the location of the boundary-layer-bleed system, relative to the terminal shock, could appreciably affect the terminal shock motion. Therefore, it is probable that the shock movement in the closed-loop tests is less than it would be if the initial shock position were closer to the aerodynamic throat. (The inlet aerodynamic throat, or forward limit of stable shock position, was located 38-3/4 inches aft of the spike vertex.) The bottom plot presents the total pressure recovery variation with time. This plot was derived by taking points on the shock position curve and assuming that the corresponding pressure recovery was that for steady-state conditions with the same shock position. From this plot a stability margin is determined which is defined as the difference in pressure recovery between the initial or steady shock position and the pressure recovery which is indicated at the farthest forward shock position. For the open-loop mode, a stability margin of approximately 1.5 counts of pressure recovery is required to prevent unstart and under closed-loop conditions about 0.1 count is required. These wind-tunnel disturbance tests do not include all the factors that may influence the terminal shock stability margin during actual flight conditions. Because of a lack of data, no provisions were made to simulate engine and structure noise, forebody turbulence, or controller time constants.

The afterburner blowout test results showed that the open-loop mode requires a stability margin of 1.2 counts of pressure recovery and the closed-loop mode requires a stability margin of about 0.4 count.

RESPONSE TO ATMOSPHERIC GUST

Figure 8 shows the response characteristics of the inlet model for both open- and closed-loop modes when the model is subjected to a simulated atmospheric gust. Note that the time scale has been considerably expanded. In the first plot, airfoil angle of attack represents the simulated atmospheric gust disturbance. This scheduled variation of airfoil angle corresponds to the measured steady-state change in local Mach number. The variation in the signal pressure, P_{12}, and the terminal shock position are shown in the next two plots. In comparing the terminal shock travel for both control modes, it will be noted that the shock motion is greater in the closed-loop mode than in the open loop. This is due to the high phase lag of the closed-loop system of which the major contributing factor is the dynamic characteristics of the bypass exit plenum. The bottom plot presents the derived pressure recovery. For this disturbance the stability margin required for both the open- and closed-loop modes is approximately 0.3 count of pressure recovery. The stability margin requirement is small because of the high frequency of this disturbance. The pressure recovery shows a large momentary decrease in recovery because of the shock passing downstream of the boundary-layer-bleed system into a high Mach number region with the attendant stronger shock — boundary-layer interaction. The downstream movement would be expected to increase the diffuser exit distortion, which, in an actual installation, might result in compressor stall. A large downstream shock movement was experienced during the afterburner blowout disturbance in the open-loop mode, which also would cause an increase in distortion.

The results of the test of a passing shock wave indicate a stability margin requirement of about 0.6 count of pressure recovery for the open-loop mode and 0.4 count for the closed-loop mode.

DESCRIPTION OF BENCH TEST SIMULATION

The second objective of the test program was to determine the dynamic and static characteristics of pressure ratio computers which might be used as inlet shock position controllers. A schematic diagram of the dynamic bench test simulation is shown in figure 9. The upper half of the diagram shows the mechanical equipment portion of the simulation which includes a pneumatic function generator to produce the desired signal pressures, a reference pressure, an actual inlet controller, the bypass actuator from the inlet model, and a simulated load on the actuator. The actuator position was transmitted to the analog computer, represented in the lower half of the diagram. This analog representation included the bypass plenum dynamics, simulated engine disturbances, the diffuser dynamics, the resultant shock position output, simulated external disturbances, and signal pressure nonlinearities. The output of the analog computer was directed into the pneumatic function generator to complete the system. Besides the dynamic characteristics of the controllers which were determined in the bench test simulation, various static characteristics were determined, such as gain, linearity, hysteresis, threshold, repeatability, saturation limits, temperature sensitivity, drift, and noise. All these measured static characteristics proved to be satisfactory and, to some degree, similar.

Significant test results obtained are shown in figure 10. The three typical controllers, designated according to their method of computing pressure ratio, are A, an electromechanical unit, B, a hydromechanical unit, and C, a hydropneumatic unit. The chart presents the ratio of closed-loop to open-loop shock travel for the three controllers for the various internal and external disturbances. The shock travel used in the ratios was the minimum travel attainable without causing an inlet unstart. Since the bench-test simulation was performed prior to the wind-tunnel test, it did not incorporate an exact representation of the inlet dynamic characteristics. In addition, a difference in initial steady-state shock position and disturbance periods contributed to the bench test shock travel distances being generally larger than those observed in the wind-tunnel test. The results shown in this chart are, therefore, indicative only of the comparative performances of the controllers. For the internal disturbances the chart shows that the performance of the three controllers was similar and generally satisfactory. The one exception, unit B during the afterburner blowout test, was due to the controller becoming saturated and thereby limiting the velocity of the bypass door. For the external disturbances, units B and C, with slower response rates than A, could not respond to the very rapid disturbances and thereby did not influence the shock travel. The ratios shown for units B and C are greater than 1.0 because the open-loop shock travel distance is very small, about the same order of magnitude as the noise in the system. Unit A, with a relatively fast response, attempted to compensate for the disturbance but only aggravated the condition because it was 180° out of phase at the disturbance frequency. This problem can easily be rectified; however, it should be recognized that such events can occur. In this case it was advantageous to have a low response controller. It should be mentioned here that these controller units were adaptations of existing hardware and additional modifications can be made to improve their response rates.

CORRELATION OF MATHEMATICAL MODEL WITH EXPERIMENTAL DATA

The final objective of the test program was to prepare a mathematical model for an analog simulation of the closed-loop wind-tunnel-test control system. This simulation was similar to that employed in the closed-loop bench test, except that all the wind-tunnel inlet model characteristics were programmed into the analog computer. The simulation was composed of an analytical model of the inlet aerodynamics and the previously measured dynamic characteristics of the bypass, controller, and signal pressure. The bypass dynamics could not be predicted purely on a theoretical basis because of the complex aerodynamic passages of the bypass exhaust system of the model used in this study; the dynamics of the controller were determined from the bench tests because they also are too complex to predict analytically; and the signal pressure dynamic characteristics from a previous wind-tunnel test were used because the analytical model could not predict the observed nonlinearities. Figure 11 shows a comparison between the results from the analog simulation and the wind-tunnel test for a closed-loop control system subjected to a throttle advance. As noted, agreement between simulated results and experiment for this case is very good. Similar results were obtained for the other internal disturbance, indicating the feasibility of conducting accurate analytical studies prior to the fabrication and test of a complete system.

CONCLUSIONS

The results obtained from this investigation indicate that for this inlet design and its idealized control system, a stability margin corresponding to a loss of less than one count of pressure recovery would prevent inlet unstart initiated by the simulated disturbances; that the dynamic and static characteristics of the current state-of-the-art inlet controllers would adequately meet the requirements of a control system for a supersonic mixed compression inlet; and analytical models can be developed which will closely correlate with experimental data.

While many useful results were obtained in this study, the need for additional research in certain areas is evident. The most important of these include:

1. Further research to better define the time history variations of pressure, temperature, and velocity in gusts and other types of atmospheric disturbances.

2. Additional research to determine the effects of dynamic inlet flow distortions on engine operation including the modeling of engine stall.

3. Additional testing of an integrated inlet-engine-exhaust system with realistic controls to further define problem areas and substantiate mathematical modeling techniques.

REFERENCE

1. Lockheed-California Company: Investigation of Supersonic Transport Engine Inlet Configuration. LR-19014, Lockheed-California Co., Sept. 30, 1965. (Prepared for NASA under Contract NAS2-2363.)

PROGRAM OBJECTIVES

- INLET DYNAMIC TESTS
- CONTROLLER BENCH TESTS
- COMPARISON OF ANALYTIC METHODS WITH RESULTS

Figure 1

INLET CONTROLS MODEL

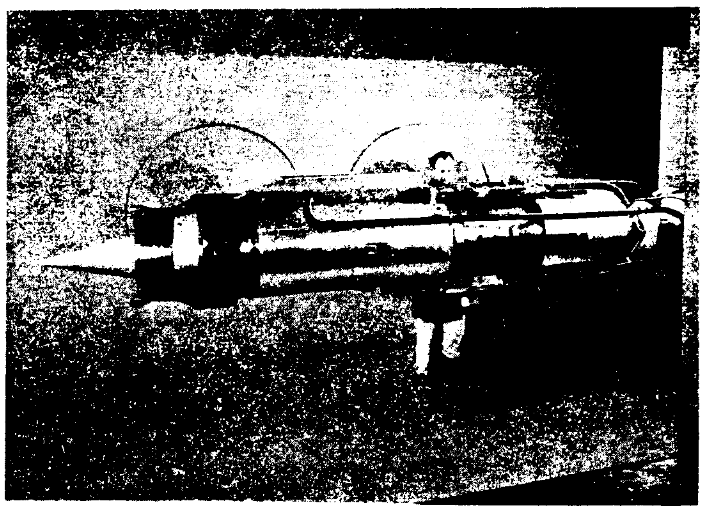

Figure 2 AAA115-2

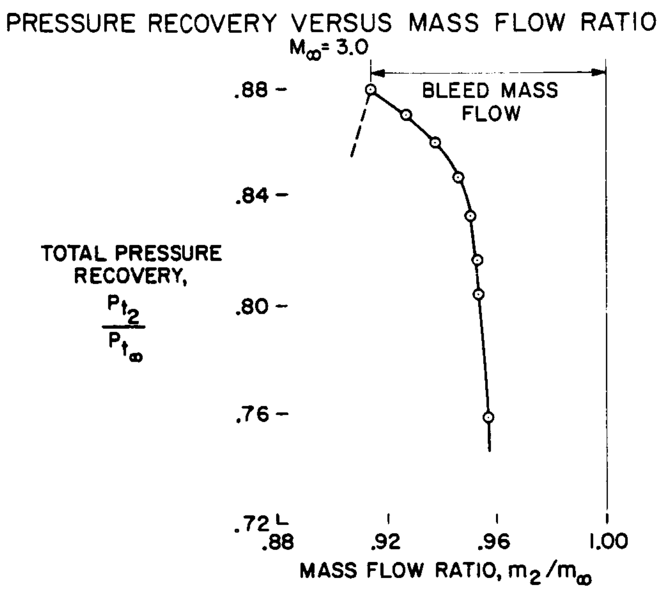

Figure 3

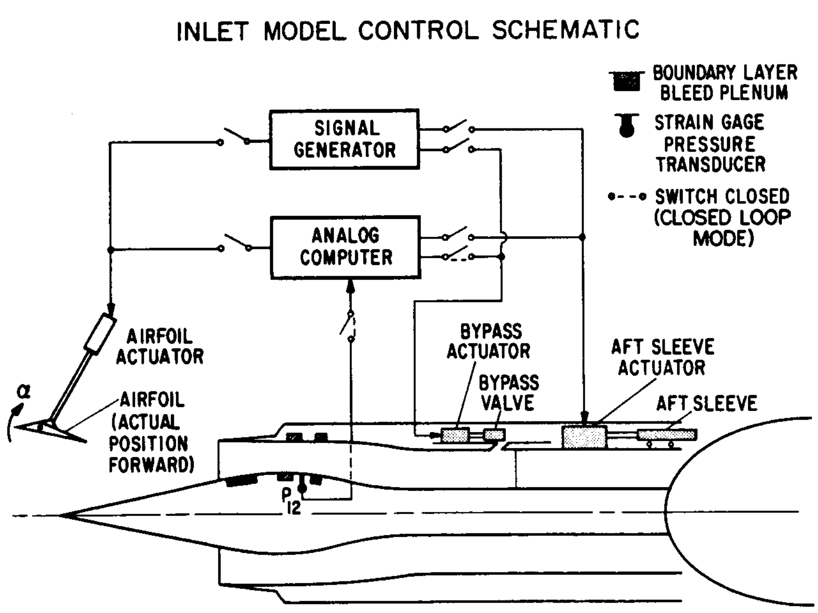

Figure 4

DISTURBANCE AIRFOIL INSTALLED IN
8× 7-ft WIND TUNNEL

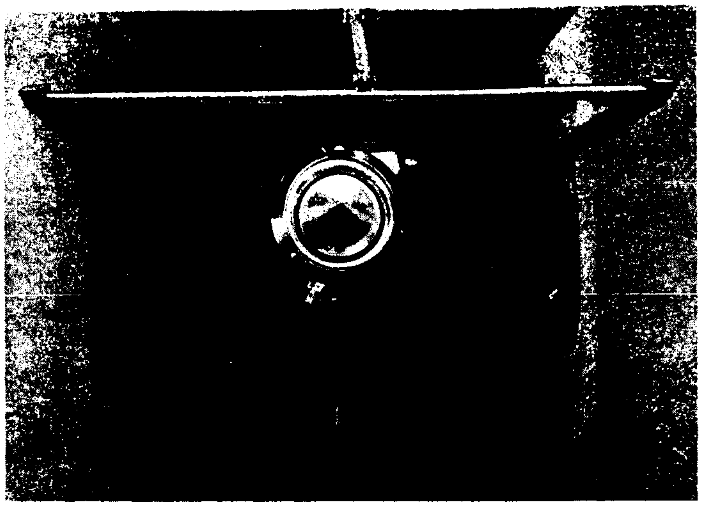

Figure 5 AAA115-5

DISTURBANCES EXAMINED

- INTERNAL DISTURBANCES
  - THROTTLE ADVANCE
  - AFTERBURNER BLOWOUT
  - SINUSOIDS — VARIOUS FREQUENCIES AND AMPLITUDES
- EXTERNAL DISTURBANCES
  - ATMOSPHERIC GUST
  - PASSING SHOCK WAVES
  - SINUSOIDS — VARIOUS FREQUENCIES AND AMPLITUDES

Figure 6

RESPONSE CHARACTERISTICS OF INLET MODEL
TO THROTTLE ADVANCE
$M_\infty = 3.0$

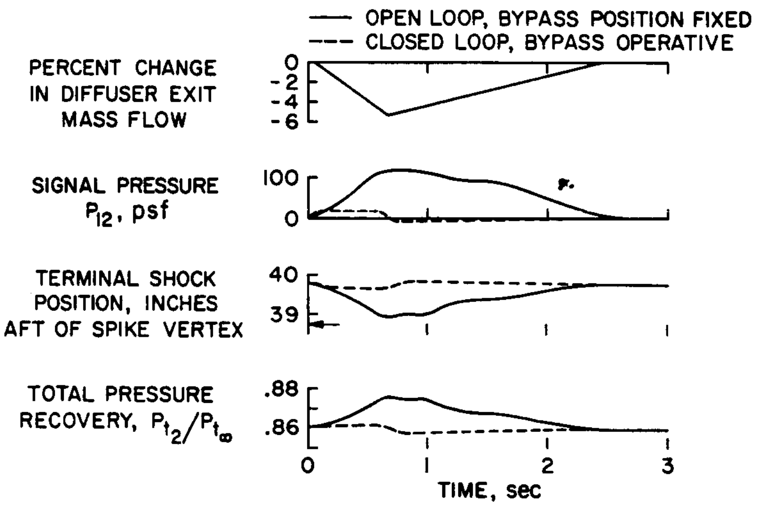

Figure 7

RESPONSE CHARACTERISTICS OF INLET MODEL
TO ATMOSPHERIC GUST
$M_\infty = 3.0$

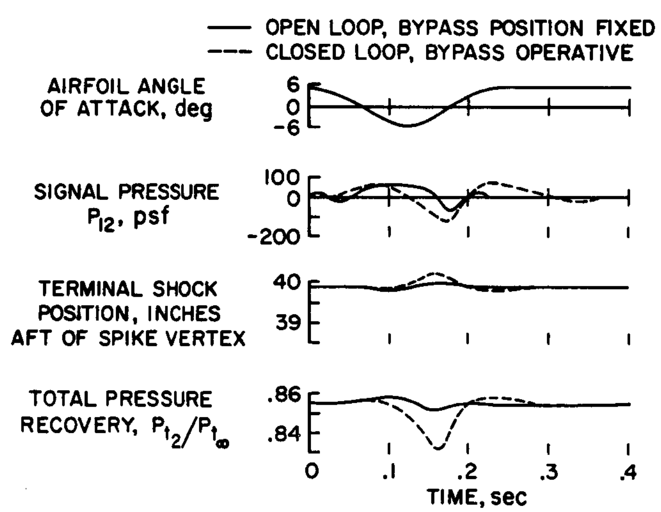

Figure 8

BENCH TEST SCHEMATIC

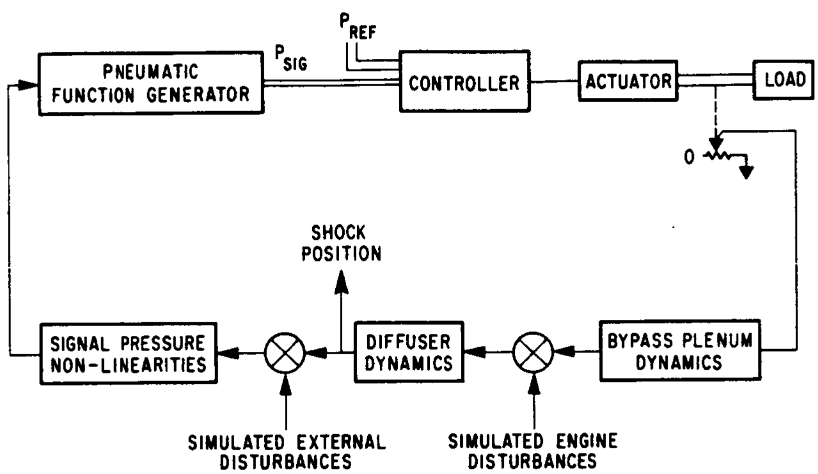

Figure 9

BENCH TEST RESULTS

	DISTURBANCE	SHOCK TRAVEL CLOSED LOOP / SHOCK TRAVEL OPEN LOOP		
		A	B	C
INTERNAL	THROTTLE ADVANCE	.6	.8	.8
	AFTER BURNER BLOW OUT	.5	1.1	.6
EXTERNAL	PASSING SHOCK WAVE	6.0	1.0	2.1
	ATMOSPHERE GUST	9.5	1.4	1.3
		ELECTRO-MECHANICAL	HYDRO-MECHANICAL	HYDRO-PNEUMATIC

Figure 10

COMPARISON OF WIND TUNNEL DATA AND ANALYTICAL SIMULATION RESULTS

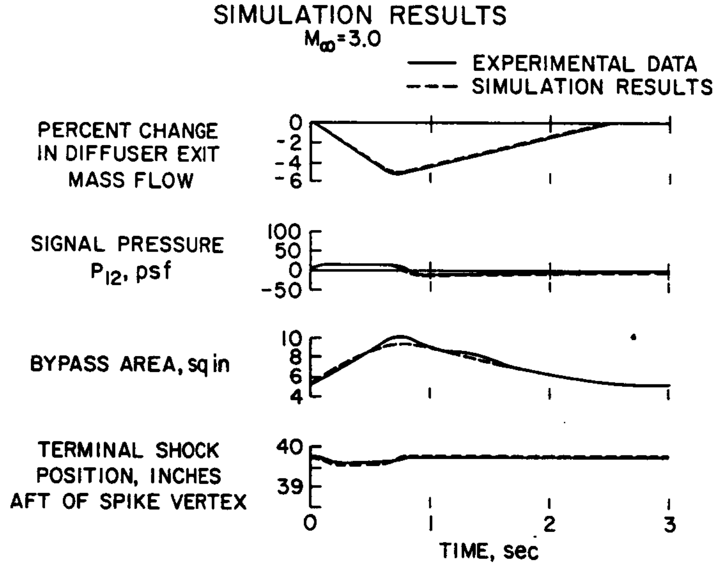

Figure 11